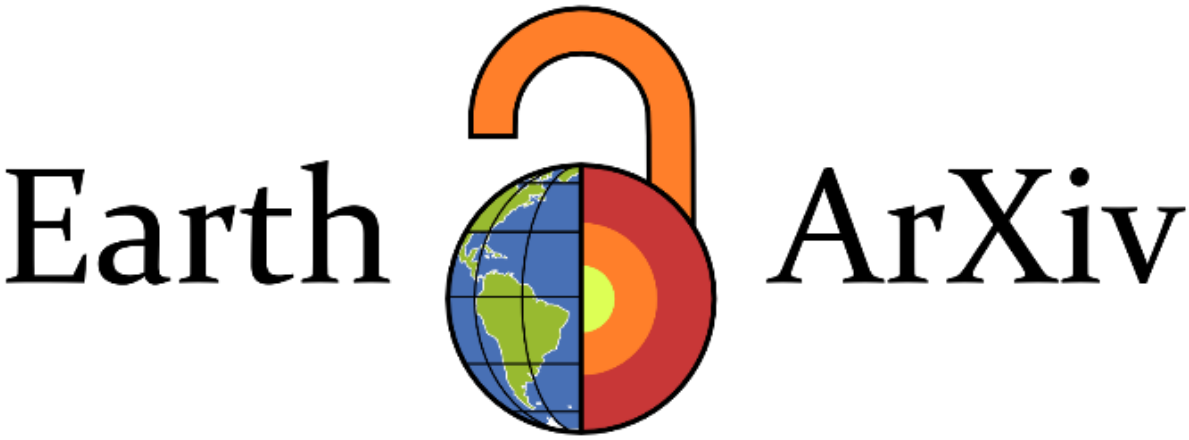

ATMOSPHERIC DEPOSITION AND SOURCE APPORTIONMENT OF MERCURY AND LEAD OVER THE LAST 150 YEARS IN HIGHLAND PEATLANDS OF SOUTHEASTERN BRAZIL

Emmanoel Vieira Silva-Filho[1*], Lúcio Fábio Lourençato[1], Andressa Cristhy Buch[1], Rut Amelia Díaz Ramos[1], Inácio Abreu Pestana[1], Vinicius Tavares Kütter[2], Eduardo Duarte Marques[3,1], Marcelo Correa Bernardes[1], Guillaume Bertrand[4], Luiz Drude Lacerda[5].

[1]Department of Geochemistry, Federal Fluminense University (UFF), Niterói, RJ, 24020-141, Brazil
[2]Geoscience Institute, Federal University of Pará (UFPA), Guamá, Belém, PA, 66075-110, Brazil
[3]Geological Survey of Brazil (SGB/CPRM), Belo Horizonte Regional Office, 30140-002, Brazil
[4]UMR CNRS UMLP 6249 Chrono-Environnement, Université Marie et Louis Pasteur, Montbéliard, France. guillaume.bertrand2@univ-fcomte.fr
[5]Laboratory of Coastal Biogeochemistry, Federal University of Ceará (UFC), Fortaleza, CE, 60165-081 Brazil

[*]**Corresponding author** – emmanoelvieirasilvafilho@id.uff.br

ABSTRACT

Trace elements like mercury (Hg) and lead (Pb) are major global pollutants subject to long-range atmospheric transport, posing a threat for human and environmental health at a global scale. Both have a great affinity with organic matter and show limited mobility in soils under stable environmental conditions. Therefore, peatlands efficiently trap and act as reliable archives of changes in anthropogenic Hg and Pb fluxes over time. This study assessed the Pb and Hg accumulation in high mountain peatlands from two Conservation Units of the Rio de Janeiro State, SE-Brazil: Itatiaia National Park - INP and Serra dos Órgãos National Park – SONP to reconstruct the history of atmospheric trace metals pollution over the last 150 years. Results indicated that in both Parks, Hg and Pb concentrations were higher from 1950s, reflecting the beginning of the industrial development in Brazil. Whereas in INP, there was a decreasing accumulation of Hg and Pb, probably due to the influence of hydrological changes since 1950s, especially. On the other hand, in SONP, both metals' accumulation rates were higher on current times (2013 to 1973) coincident with the increase in these elements' emissions to the atmosphere in South America. The Hg enrichment factors (EF) were 215 and 130 for INP and SONP respectively, whereas the Pb EF values were 47.4 in INP and 24.7 in SONP. Such evidence indicates a current need for more effective environmental policies and guidelines to control emissions to the atmosphere of these two environmentally significant pollutants.

Keywords: Accumulation rate; anthropogenic emissions; Enrichment factor; Peat core; Trace elements.

1. INTRODUCTION

Human activities have significantly increased metal use in various industries leading to their release into the environment and causing toxic effects (Watari et al., 2021). Among these metals, mercury (Hg) and lead (Pb) are of particular concern due to their high toxicity (WHO, 2021; Taylor et al., 2019; Zhang et al., 2019). Metals enter the atmosphere from both natural sources, such as volcanic eruptions, geothermal springs, geologic deposits, the weathering of rocks and soils, forest fires, degassing from oceans, and human activities, including fossil fuel combustion and industrial processes. When these anthropogenic metallic aerosols mix with natural aerosols, they can become more readily deposited in soils (Moteki et al., 2017). While volcanic eruptions and natural processes still contribute significantly to Hg and Pb total emission to the environment, human activities like fossil fuel combustion and industrial processes became their major sources after industrialization. These emissions are transported globally through the atmosphere, with projections suggesting a decrease in deposition in the Northern Hemisphere but an increase in the Southern Hemisphere. This trend may be linked to the observed four-fold rise in Hg concentration within the surface ocean over the past 600 years, for example (Pacyna et al., 2009; Sigel et al., 2017; Zhang et al., 2014). Studies on sediments, ice cores and peatlands reveal a concerning trend of increasing Hg deposition that has tripled since pre-industrial times (Lindeberg et al., 2007). In the case of Pb, the main sources to the atmosphere have been industry, mostly coal burning, ferrous and nonferrous smelting, and open waste incineration until ~1950. After, most significant Pb source was *leaded* motor vehicle gasoline use since World War II, resulting in the largest Pb emissions to the atmosphere between 1950 and 1980, related to traffic exhaust. From the 1980's thereafter Pb fluxes to the atmosphere decreased sharply due to the phasing out of leaded motor vehicle gasoline (Weiss et al., 1999), and this trend has occurred in both hemispheres (Lacerda and Ribeiro, 2004). Climate change is expected to exacerbate this issue by further increasing the remobilization of deposited metals from terrestrial and marine surfaces (Li et al., 2020). This is particularly worrisome in the case of Hg, because methyl-Hg, its most toxic form, can bioaccumulate in the food chain, posing a significant threat to ecosystems and human health (Buch et al., 2018).

Despite government regulations, environmental pollution from Hg and Pb, like other heavy metals, remains a global concern. Estimates of global anthropogenic Hg emissions vary widely, ranging from 2,700 to 7,500 tons per year (Lacerda, 2003; De Jesus et al., 2018). The US Environmental Protection Agency (USEPA) estimates annual

global anthropogenic emissions at approximately 2,220 metric tons per year, with South America contributing approximately 18.4% (AMAP, 2018). Despite recent advancements, significant uncertainties remain in these estimates, with a range of 1,010-4,070 tons per year (UNEP, 2013). Globally, Pb emissions decreased sharply after the the phasing out of Pb in motor vehicle gasoline. However, recent trends in Pb usage and recycling suggest an estimated emission of $2.84.10^6$ t of Pb were discharged into the environment in 2000, in 2022 this emission nearly doubled reaching about 5.10^6 t. (Luby et al., 2024).

Understanding the history of Hg and Pb deposition in remote areas like Southeast Brazil is crucial to assess its long-term environmental impact. Peat cores, which act as natural archives of atmospheric deposition, can provide valuable insights into historical trends. Although peatlands have been used extensively to reconstruct atmospheric metal deposition in boreal and temperate regions (Shotyk et al., 2002 and 2016; Martínez-Cortizas et al., 1999), research using tropical peat records remains scarce (Page et al., 1999; Anshari et al., 2001; Wüst and Bustin, 2004; Lacerda and Ribeiro, 2004; Cooke et al., 2021). In this sense, this study aimed to reconstruct the historical atmospheric deposition of Hg and Pb for the last 150 years, archived in two tropical peat cores in Southeast Brazil.

2. MATERIAL AND METHODS

2.1 Sampling area

The study was conducted in two Conservation Units of Rio de Janeiro State, southeastern Brazil: Itatiaia National Park – INP (22°17'57" S; 44°37'15" W; 1,888 m a.s.l.) and Serra dos Órgãos National Park – SONP (22°27'32" S; 43°01'37" W; 2,117 m a.s.l.) (Figure 1). The parks were selected due to their elevation range (resulting in cool, humid climates with mean annual temperatures of 10–15°C) and differing precipitation regimes (2,500 mm yr^{-1} at INP; 3,600 mm yr^{-1} at SONP) (Nimer, 1979). Both areas have low anthropogenic impact and preserve ombrotrophic peatlands fed exclusively by atmospheric inputs, making them ideal for establishing background levels of potentially toxic elements and reconstructing historical atmospheric deposition.

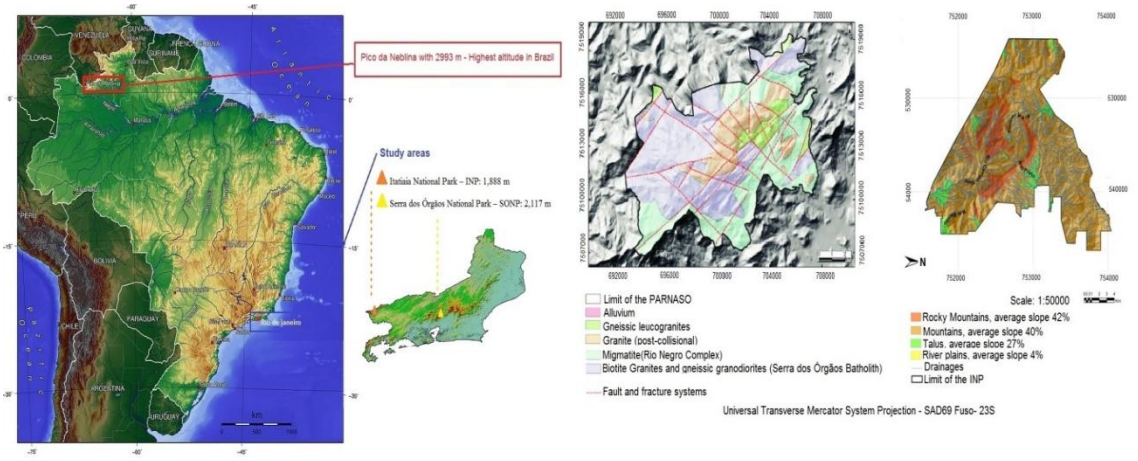

Figure 1. Location map of the study areas in southeastern Brazil. (a) Geographic position of Rio de Janeiro State within Brazil; (b) detailed view of the two Conservation Units: Itatiaia National Park (INP) and Serra dos Órgãos National Park (SONP).

2.2 Peat Core Collection Sample Handling and Storage

Peat cores were collected using a 100 cm long and 10 cm diameter core sampler. The sampler was manually introduced from the soil surface into the basal peat layer (Figure 2). The core collection depth varied between the two sites: Itatiaia National Park (INP) reached up to 41 cm, while Serra dos Órgãos National Park (SONP) had a maximum depth of 30 cm. The depth of peat core collection was determined by several factors, including logistical considerations, research objectives, and anticipated peat depth. A ~50 cm depth was sufficient to capture recent historical trends in metal deposition and assess anthropogenic impacts. Once collected, each peat core was sectioned at a resolution of 1.5 cm. To preserve the integrity of the samples, the 1.5 cm peat slices were placed in a thermal box and kept refrigerated during transport to the laboratory. Upon arrival, the samples were stored in a freezer until further analysis.

Figure 2. Ombrotrophic peatland sampling sites. (a) Itatiaia National Park (INP, 22°17'57" S; 44°37'15" W; 1,888 m a.s.l.); (b) Serra dos Órgãos National Park (SONP, 22°27'32" S; 43°01'37" W; 2,117 m a.s.l.). The peatlands are located within high-altitude grasslands (*campo de altitude*) and receive water and nutrients exclusively from atmospheric deposition, making them suitable natural archives for reconstructing historical inputs of Hg, Pb, and other potentially toxic elements.

2.3 Chemical analysis

2.3.1 Peat characterization parameters

Prior to mercury (Hg), lead (Pb), and titanium (Ti) analysis, the peat samples were characterized for unrubbed fiber (UF), rubbed fiber (RF), solubility in sodium pyrophosphate, pH in $CaCl_2$, soil bulk density (SBD), organic matter density (OMD), mineral material (MM), organic matter (OM), and gravimetric moisture (GM), according to Lynn et al. (1974). These parameters provided fundamental information on peat decomposition degree, organic matter provenance, and mineral input, which are essential for interpreting trace element concentrations in the context of atmospheric deposition. Total organic carbon (TOC) and total nitrogen (N) were determined by dry combustion using a Perkin-Elmer CHNS/O Analyzer 2400, with acetanilide as the calibration standard.

2.3.2 Mercury analysis

For the determination of total Hg concentration, approximately 1.0 g of freeze-dried samples were weighed and subjected to acidic extraction using aqua regia (3:1 mixture of $HCl:HNO_3$ (v/v), both suprapure) at 70°C in a closed cold-finger system (Malm et al.,

1990). Mercury (Hg) determination was performed using Cold Vapor Atomic Absorption Spectrophotometry (CVAAS) with a Bacharach Coleman Model 50d mercury analyzer. In this method, Hg^{2+} ions are reduced to volatile Hg^0 using $SnCl_2$ (Marins et al., 1998), which is then quantified by the CVAAS instrument.

2.3.3 Lead and titanium analysis

Freeze-dried peat samples (0.2-0.3 g dry weight) were processed for Pb and Ti analysis using a microwave digester (speedwave™ MWS-3+; Bergof). Each sample was digested with 6 ml of 65% HNO_3 (Merck suprapure) following a food-grade temperature program (100-170 °C). After cooling, the digested samples were diluted with deionized water to a final volume of 25 ml. Concentrations of Pb and Ti were then determined by Inductively Coupled Plasma Optical Emission Spectrometry (ICP-OES).

2.3.4 Quality control

To ensure the accuracy of the analysis, blanks and replicates were included in each analytical batch. Additionally, a certified reference material (SRM 2709a San Joaquin Soil, National Institute of Standards and Technology-NIST) was incorporated to assess the digestion process effectiveness. The recovery for this reference material ranged from 82% to 92% (Table 1). The detection limit was calculated as 3 times the standard deviation of the blank measurements.

Table 1. Analytical quality control data for mercury (Hg), lead (Pb), and titanium (Ti) measurements, including reference values (SRM 2709a - NIST), mean measured values (n = 8), reproducibility (%), and detection limits.

Element	Reference values	Mean measured values (n = 8)	Recovery (%)	Detection limit (n = 8)
Hg (mg kg^{-1})	0.9 ± 0.2	0.73 ± 0.1	82	0.004
Pb (mg kg^{-1})	17.3 ± 0.1	15.2 ± 13.5	88	0.01
Ti (%)	0.336 ± 0.007	0.309 ± 0.614	92	0.001

2.4 Data analysis

2.4.1 Trace metal accumulation rates

Trace metal accumulation rates (AR) were calculated for Hg and Pb using the equation (Eq. 1) established by Roos-Barraclough et al. (2002, 2006) and Givelet et al. (2003).

$$AR\ (mg\ m^{-2}\ y^{-1}) = 10 \times [E]\ (\mu g\ g^{-1}) \times D\ (g\ cm^{-3}) \times SR\ (cm\ y^{-1}) \quad \text{Eq. 1}$$

Where, AR represents the accumulation rate, [E] is the measured metal concentration (μg g^{-1}), D is the peat density (g cm^{-3}), and SR is the sedimentation rate (cm y^{-1}).

2.4.2 Enrichment factors

Enrichment factors (EF) for Hg and Pb were determined using the formula from Shotyk et al. (2002):

EF = ([E]sample / [Ti]sample) / ([E]crust / [Ti]crust)

Here, EF represents the enrichment factor, [E]sample is the concentration of the trace element in the sample (μg g^{-1}), [Ti]sample is the titanium concentration in the sample (μg g^{-1}), [E]crust is the reference concentration of the trace element in the Earth's crust (μg g^{-1}), and [Ti]crust is the reference concentration of titanium in the Earth's crust (μg g^{-1}).

Since local reference concentrations for Hg and Pb were unavailable, crustal reference values from Wedepohl (1995) were employed.

2.4.3 Lithogenic background estimation

To estimate the lithogenic contribution (natural background) to the total Hg and Pb concentration, the following equation based on Shotyk et al. (2000) (Eq. 2)

[E lithogenic] = [Ti] sample × ([E]crust / [Ti] crust) Eq. 2

In this equation, [E lithogenic] represents the estimated lithogenic Hg or Pb concentration (μg g^{-1}), [Ti] sample is the titanium concentration in the sample (μg g^{-1}), [E]crust is the reference concentration of Hg or Pb in the Earth's crust (μg g^{-1}), and [Ti] crust is the reference concentration of titanium in the Earth's crust (μg g^{-1}).

2.4.4 Statistical Analyses

All statistical analyses were performed in the R environment (R Core Team, 2024) using the RStudio interface (Posit Team, 2024). Descriptive statistics (mean, median, standard deviation, minimum, maximum, and coefficient of variation) were calculated for each variable (peat characterization parameters, Hg, Pb, Ti, TOC, and N) per study area.

A Principal Component Analysis (PCA) was conducted to explore the relationships among variables and to assess differences in geochemical signatures between Itatiaia National Park (INP) and Serra dos Órgãos National Park (SONP). Prior to PCA, the data were normalized (mean-centered and scaled to unit variance) using the prcomp function from the stats package (R Core Team, 2024). The results were visualized using the first

two principal components, which together explained 69.4% of the total variance (to be filled in Results), employing the ggbiplot function (ggbiplot package, Vu, 2011). To evaluate whether the two areas occupy distinct multivariate spaces, 95% confidence ellipses were drawn around the centroid of each study area.

2.5. Sedimentation rates and chronology

2.5.1 ^{210}Pb Dating

Lead-210 (^{210}Pb) activity was measured to establish sedimentation rates and develop a chronology for the peat cores. This method is widely used for peat studies because it assumes minimal post-depositional remobilization of trace metals once deposited (Mróz et al., 2017). ^{210}Pb activity was determined using gamma spectrometry with a high-purity germanium well detector (Canberra) coupled to a multichannel analyzer (Cutshall et al., 1983). Refer to Lourençato et al. (2017) for further details on the radioisotope dating procedure employed.

2.5.2. Sedimentation rate calculation

The Constant Initial Concentration (CIC) model developed by Appleby and Oldfield (1983) was used to calculate accumulation rates (AR) based on the ^{210}Pb activity profiles. Sedimentation rate (SR) was then determined using the following equation:

$$SR\ (cm\ y^{-1}) = \lambda / S$$

Where:

SR is the sedimentation rate (cm y^{-1}), λ is the decay constant of ^{210}Pb (0.0307 y^{-1}), S is the slope of the linear regression of depth plotted against the logarithm of unsupported ^{210}Pb activity (Bq g^{-1}).

2.5.3. Peat accumulation rate

The peat accumulation rate (PAR) was calculated using the following equation:

$$PAR\ (g\ cm^{-2}\ y^{-1}) = SR\ (cm\ y^{-1}) \times BD\ (g\ cm^{-3})$$

where:

PAR is the peat accumulation rate (g cm^{-2} y^{-1}), SR is the sedimentation rate (cm y^{-1}), BD is the bulk density of the peat (g cm^{-3}).

3. RESULTS

The peat soils from both INP and SONP were classified as Typical Haplosaprist Histosols according to the Embrapa classification system (2013) (Figure 2). The dominant

plant family identified at the peat surface was Poaceae, with additional presence of families such as Myrtaceae, Asteraceae, Euphorbiaceae, Rubiaceae, Leguminosae, Cyperaceae, and Bromeliaceae (identification source: ICMBio, 2013a, 2013b). The peat samples displayed a dark color, with an average Munsell Soil Color Chart value of 3 for brightness and 2 for Chroma.

The pH measured in $CaCl_2$ solution were extremely acidic, ranging from an average of 2.43 to 3.78. The average unrubbed and rubbed fiber contents were 60% and 19%, respectively. Gravimetric moisture content exceeded 200% in most peat samples. The average nitrogen content was 0.44 ± 0.26% in INP and 0.45 ± 0.14% in SONP, whereas the average total organic carbon content was 12.69% in INP and 23.34% in SONP.

The vertical distribution of ^{210}Pb activity in both INP and SONP peat profiles exhibited a relatively well-defined exponential decrease with depth (Figure 3A). This pattern is consistent with the distribution typically observed in natural sediments (Appleby and Oldfield, 1983). In simpler terms, the ^{210}Pb activity generally decreased with deeper peat layers. However, it's important to note that subsurface layer (2-4 cm) of both cores showed slightly higher ^{210}Pb values compared to the top layers (0-2 cm).

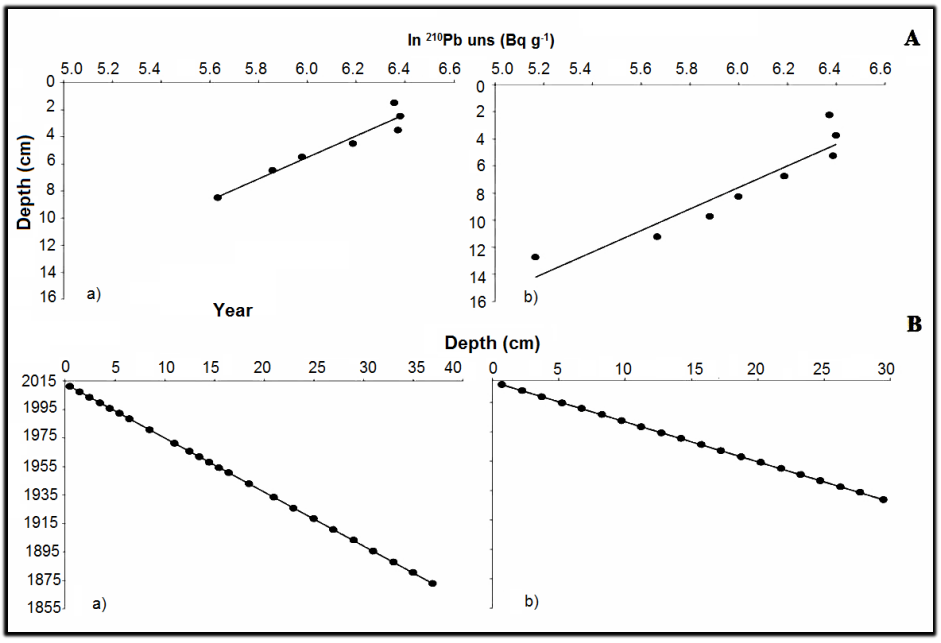

Figure 3. **A)** Excess ^{210}Pb activity (calculated using the constant flux model) as a function of depth (cm) for peat cores from (a) Itatiaia National Park (INP) and (b) Serra dos Órgãos National Park (SONP). **B)** Age-depth models derived from linear interpolation between ^{14}C and ^{210}Pb dating points for (a) INP and (b) SONP.

The chronology reconstructed using the ^{210}Pb profile from INP (41 cm depth) indicated a peat accumulation rate of 0.18 g m^{-2} y^{-1} starting from 1861 (Figure 3B). This rate decreased to an average of 0.08 g m^{-2} y^{-1} around 1950. In contrast, the SONP peat profile (30 cm depth) displayed a more constant peat accumulation rate of 0.10 g m^{-2} y^{-1} throughout the profile, with deposition starting around 1934 (Figure 3B). The average sedimentation rates determined using ^{210}Pb were 0.26 cm y^{-1} for INP and 0.37 cm y^{-1} for SONP (Figure 3B).

Table 2 provides a statistical summary of the measured parameters in peat profiles from INP and SONP. As a lithogenic element derived from bedrock weathering, titanium (Ti) concentrations varied considerably between the two parks, reflecting their distinct geological substrates. INP, underlain by Precambrian alkaline intrusive rocks (Silva Rosa & Ruberti, 2018), exhibited Ti concentrations ranging from 24.4 to 62.1 µg g^{-1} (mean: 45.7 ± 10.8 µg g^{-1}). In contrast, SONP, situated on Precambrian granitoid gneisses (Fernandes et al., 2022), displayed a wider range of Ti concentrations (17.9–132.0 µg g^{-1}; mean: 82.1 ± 36.6 µg g^{-1}). Interestingly, despite its lithogenic origin, Ti concentrations decreased in the surface layers of both peatlands, suggesting either dilution by organic matter accumulation or post-depositional mobilization. In INP, this decrease began around the 1990s (depth < 5 cm), while in SONP, it started earlier, around the 1970s (depth < 15.75 cm). These divergent temporal trends may reflect differences in peat accumulation rates, organic matter inputs, or hydrological regimes between the two sites. Notably, while Ti concentrations decreased toward the surface in both peatlands, Hg concentrations showed the opposite trend, increasing significantly in recent decades (Table 2; Figures 4 and 5). This inverse relationship further supports the interpretation that Hg is derived primarily from atmospheric deposition rather than lithogenic sources or soil erosion. Having established the contrasting behavior of Ti between the two parks, we now examine the temporal trends and enrichment patterns of Hg and Pb, the primary pollutants of interest in this study.

Table 2. Statistical summary (median, mean, standard deviation, minimum, and maximum) of the measured parameters in peat profiles from Itatiaia National Park (INP) and Serra dos Órgãos National Park (SONP), southeastern Brazil. Parameters include bulk density, total mercury (Hg) and lead (Pb) concentrations, accumulation rates (AR) for Hg and Pb, titanium (Ti) concentrations, lithogenic fractions (Hg Lit and Pb Lit), and enrichment factors (EF Hg and EF Pb). Hg AR is expressed in μg m^{-2} yr^{-1}; Pb AR is expressed in mg m^{-2} yr^{-1}. Lithogenic fractions represent the estimated contribution from local rock weathering. Enrichment factors were calculated using Ti as the reference element, following [referência utilizada, ex.: Shotyk et al., 1998].

INP	**Median**	**Mean**	**Std. Dev.**	**Minimum**	**Maximum**
Bulk Density (g cm^{-3})	0.49	0.52	0.19	0.27	0.79
Hg (ng g^{-1})	158.4	162.2	28.7	110.5	219.4
Hg AR (μg m^{-2} yr^{-1})	**203.3**	**210.2**	**59.2**	**133.4**	**311.4**
Pb (μg g^{-1})	12.2	11.1	2.5	6.6	15.6
Pb AR (mg m^{-2} yr^{-1})	14.8	14.8	4.9	6.3	24.9
Ti (μg g^{-1})	48.5	45.7	10.8	24.4	62.1
Hg Lit (ng g^{-1})	1.2	1.1	0.3	0.6	1.5
EF Hg	191.5	215.0	86.5	95.3	429.4
Pb Lit (μg g^{-1})	0.2	0.3	0.1	0.2	0.3
EF Pb	42.5	47.4	13.4	27.7	68.7
SONP	Median	Mean	Std. Dev.	Minimum	Maximum
Bulk Density (g cm^{-3})	0.5	0.5	0.2	0.3	0.8
Hg (ng g^{-1})	156.9	155.6	30.1	102.5	202.7
Hg AR (μg m^{-2} yr^{-1})	**189.5**	**186.0**	**40.3**	**103.8**	**250.9**
Pb (μg g^{-1})	9.3	9.6	2.0	5.0	13.1
Pb AR (mg m^{-2} yr^{-1})	10.0	10.1	2.1	5.3	13.9
Ti (μg g^{-1})	85.7	82.1	36.6	17.9	132.0
Hg Lit (ng g^{-1})	1.5	1.5	0.7	0.3	2.4
EF Hg	114.6	130.0	66.2	50.3	321.4
Pb Lit (μg g^{-1})	0.5	0.5	0.2	0.1	0.7
EF Pb	23.9	24.7	14.3	10.2	64.3

Notes: AR = accumulation rate. Hg AR is presented in μg m^{-2} yr^{-1}; Pb AR is presented in mg m^{-2} yr^{-1}. EF = enrichment factor (calculated using Ti as the reference element). Lit = lithogenic fraction.

The vertical distribution of Ti, Hg, Pb, and derived parameters in the INP peat core is presented in Figure 4, revealing distinct trends that reflect both anthropogenic inputs and natural processes. Concentrations of Hg in the INP peat profile ranged from 110.5 ng g^{-1} to 219.4 ng g^{-1}, with a mean of 162.2 ± 28.7 ng g^{-1} (Figure 4).

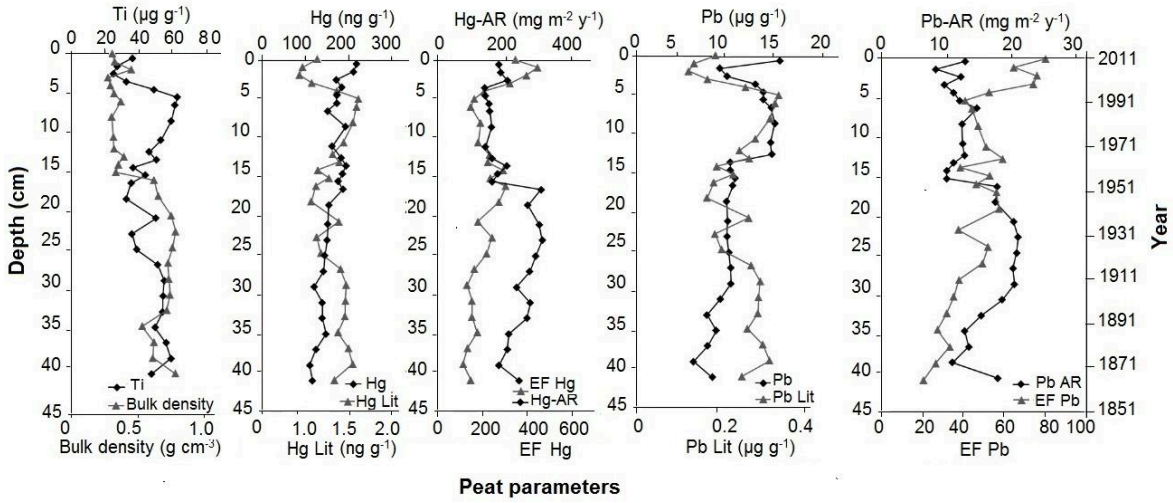

Figure 4. Depth profiles of bulk density, Ti, HgLit, HgT, EF Hg, Hg AR, PbLit, PbT, EF Pb, and Pb AR in the INP peat core. Depths (cm) and corresponding ages (^{210}Pb dating) are shown on the left axis. Units: bulk density (g cm^{-3}); Ti (µg g^{-1}); Hg (ng g^{-1}); Hg AR (µg m^{-2} yr^{-1}); Pb (µg g^{-1}); Pb AR (mg m^{-2} yr^{-1}).

Similarly, Hg concentrations in the SONP profile varied between 102.5 ng g^{-1} and 202.7 ng g^{-1}, with a mean value of 155.6 ± 30.1 ng g^{-1} (Figure 5). Lead (Pb) concentrations ranged from 5.0 to 13.1 µg g^{-1} (mean: 9.6 ± 2.0 µg g^{-1}), while titanium (Ti) concentrations varied between 17.9 and 132.0 µg g^{-1} (mean: 82.1 ± 36.6 µg g^{-1}). Enrichment factors confirmed severe anthropogenic enrichment for both metals, with mean EF Hg of 130.0 ± 66.2 and mean EF Pb of 24.7 ± 14.3. Lithogenic fractions were negligible for both elements (Hg Lit: 0.3–2.4 ng g^{-1}; Pb Lit: 0.1–0.7 µg g^{-1}), further supporting an atmospheric origin for the observed enrichment.

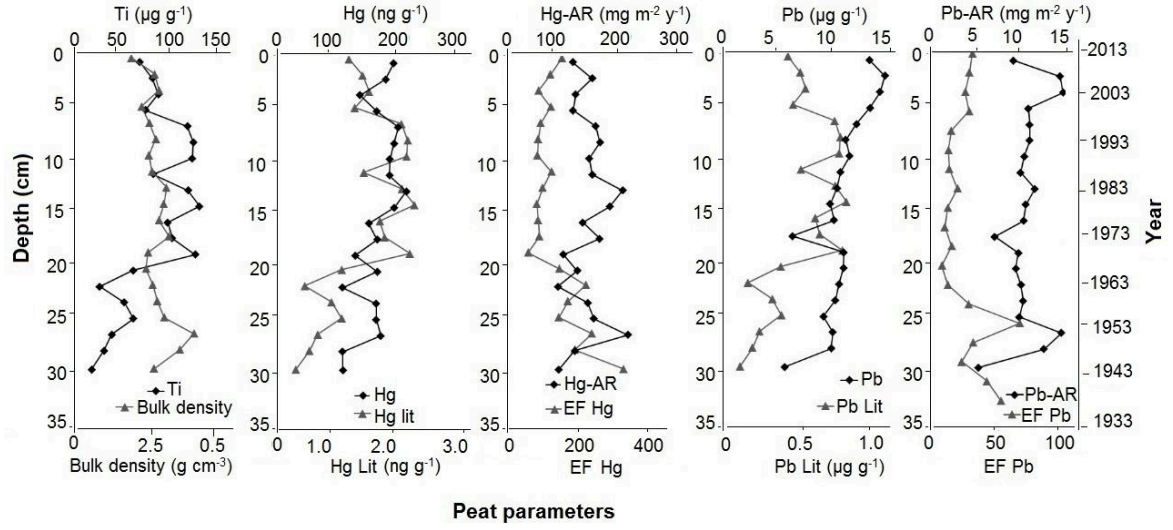

Figure 5. Depth profiles of bulk density, Ti, HgLit, HgT, EF Hg, Hg AR, PbLit, PbT, EF Pb, and Pb AR in the SONP peat core. Depths (cm) and corresponding ages (^{210}Pb dating) are shown on the left axis. Units: bulk density (g cm^{-3}); Ti (µg g^{-1}); Hg (ng g^{-1}); Hg AR (µg m^{-2} yr^{-1}); Pb (µg g^{-1}); Pb AR (mg m^{-2} yr^{-1}).

Both INP and SONP profiles exhibited higher Hg concentrations in the top 18.5 cm and 15.5 cm layers, respectively. These upper layers, corresponding to the post-1950s period, showed average Hg concentrations of 179.9 ± 19.5 ng g^{-1} (INP) and 175.2 ± 20.1 ng g^{-1} (SONP). In contrast, deeper layers (pre-1950s) had lower average Hg concentrations of 137.2 ± 15.2 ng g^{-1} (INP) and 136 ± 25 ng g^{-1} (SONP). This trend likely reflects increased anthropogenic Hg emissions and deposition during the post-industrial era, highlighting the potential ecological and human health risks associated with Hg pollution.

The average Hg accumulation rate in the INP peat profile was 210.2 ± 59.2 mg m^{-2} y^{-1}, with a range of 133.4 to 311.4 mg m^{-2} y^{-1} (Figure 4). Notably, despite higher Hg concentrations in surface layers, the accumulation rate was lower at the surface and increased with depth. The SONP peat profile displayed a similar trend. The average Hg accumulation rate was 186 ± 40.3 mg m^{-2} y^{-1}, with a range of 103.8 to 250.9 mg m^{-2} y^{-1} (Figure 5). In addition, the Hg accumulation rate was higher in the surface layers (176.3 ± 33.9 mg m^{-2} y^{-1}) compared to deeper sections (155.4 ± 45.0 mg m^{-2} y^{-1}).

Concentrations of Pb in the INP peat profile displayed a similar trend to Hg, with higher values observed in surface layers compared to deeper sections (Figure 4). Lead concentrations ranged from 6.6 to 15.6 µg g^{-1}, with an average of 11.1 ± 2.5 µg g^{-1}. The highest Pb concentration (13.6 ± 2.3 µg g^{-1}) was found in the surface layer (around 12.5 cm depth), corresponding to the mid-1960s. In contrast, deeper sections (below 12.5 cm) exhibited a lower average Pb concentration of 9.6 ± 1.2 µg g^{-1}. The SONP peat profile showed a decreasing trend in Pb concentration with depth (Figure 5). Lead concentrations ranged from 5.0 to 13.1 µg g^{-1}, with an average of 9.6 ± 2.0 µg g^{-1}. Interestingly, the Pb accumulation rate (AR) in the INP peat profile was lower in the surface layers compared to deeper sections. Surface layers (above 12.5 cm depth) had an average Pb AR of 12.6 ± 3.3 mg m^{-2} y^{-1}, while deeper layers displayed a higher average Pb AR of 17.3 ± 3.5 mg m^{-2} y^{-1}. The Pb AR in the SONP peat profile remained relatively constant (average of 10.1 ± 2.1 mg m^{-2} y^{-1}) throughout the profile, except for three specific depths (2.25, 3.75, and 26.75 cm) where higher Pb AR values (13.6, 13.9, and 13.7 mg m^{-2} y^{-1}, respectively) were observed.

The Hg enrichment factor (EF) was higher than the Pb EF in both INP (Hg EF = 215, Pb EF = 47) and SONP (Hg EF = 130, Pb EF = 25). Both Hg and Pb exhibited a decrease in the lithogenic fraction with increasing depth in both peat profiles (Figures 4

and 5). This trend was disrupted only in the uppermost layers (less than 5 cm), where a decrease in the overall concentration of both elements was observed.

Despite the similar behavior patterns of Hg and Pb observed in the PCA (Figure 6: variables HgLit and PbLit), the contribution of lithogenic Pb to total Pb concentration in the peat was more significant than that of lithogenic Hg. The mean percentage of lithogenic Pb relative to total Pb was 2.4% in INP and 4.8% in SONP. In contrast, the mean percentage of lithogenic Hg relative to total Hg was only 0.5% in INP and 1.0% in SONP. These results indicate that atmospheric deposition is the dominant source of both elements, with a negligible lithogenic influence for Hg and a minor contribution for Pb, particularly in SONP.

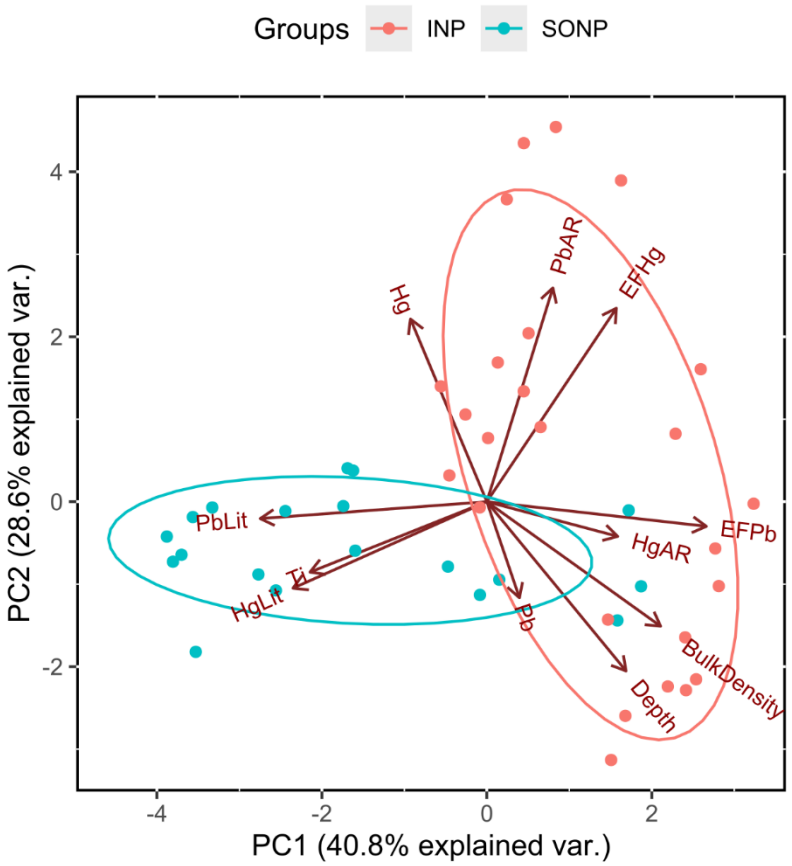

Figure 6. Principal Component Analysis (PCA) biplot of the geochemical variables measured in peat samples from Itatiaia National Park (INP, red) and Serra dos Órgãos National Park (SONP, blue). The first two principal components (PC1 and PC2) explain 69.4% of the total variance. Ellipses represent 95% confidence intervals around the centroid of each study area. Vectors indicate the contribution of each variable (Hg, Pb, Ti, TOC, N, OM, SBD, pH in $CaCl_2$, MM, GM, UF, RF, and pyrophosphate solubility) to the principal components. The angle and length of each vector indicate the correlation and contribution strength, respectively.

Given the low lithogenic contributions observed, the following section discusses the historical trends of atmospheric Hg and Pb deposition recorded in the peat profiles of INP and SONP

4. DISCUSSION

The significant increase in Hg and Pb accumulation rates observed in the INP peat profile after the 1950s warrants further investigation (Figure 4). This pattern might be linked to climate changes influencing biogeochemical processes in the peatland, as previously documented for this region (Groissman et al., 2005; Marengo et al., 2009). Hydrological conditions play a crucial role in peatland development and metal accumulation. Changes in precipitation patterns, evapotranspiration rates, and water table levels can significantly influence the rate of peat accumulation, decomposition rates, and the transport of metals within the peatland system (Taminskas et al., 2018). As reported by Lourençato et al. (2017, 2019), a decrease in peat accumulation rates in this region has been linked to a reduction in bulk density, associated with increased frequency and intensity of extreme rainfall events since the 1950s.

Increased precipitation can lead to higher water table levels, promoting peat accumulation and reducing decomposition rates. However, extreme rainfall events can also cause erosion and transport of sediments and associated metals into the peatland.

Decreased precipitation or increased evapotranspiration can lower the water table, leading to increased decomposition rates and reduced peat accumulation. This may also result in the oxidation of previously reduced metals, making them more mobile and susceptible to leaching.

Alterations in hydrological conditions can affect the redox conditions within the peatland, influencing the speciation and mobility of metals. For example, fluctuating water levels can lead to cycles of oxidation and reduction, which can affect the bioavailability and toxicity of metals. Mesocosm experiments have demonstrated that hydrological changes, such as water table fluctuations, can significantly impact peatland dynamics, including decomposition rates and carbon accumulation (Barel et al., 2021). These findings are consistent with observations from other tropical peatland systems, including the work of Lourençato et al. (2017). While climate change is likely a major driver of these changes, human activities, such as deforestation and pollution, may also contribute to altered hydrological regimes and increased metal deposition. Further

research is needed to fully elucidate the complex interplay between climate change, human activities, and peatland ecosystem processes.

Titanium (Ti) is widely used as a geochemical normalizer due to its minimal response to water table fluctuations and biological processes (Nieboer, 1982; Hausmann et al., 2018). Accordingly, our data show no correlation between Ti and either Hg or Pb (Figure 6). In peatlands, increasing Ti content often reflects broader landscape changes, such as soil erosion linked to land-use practices or climatic variability (Küttner et al., 2014). The observed increase in Ti concentration within the INP peat profile from the 1950s onwards (Figure 4) coincides with the reported intensification of extreme rainfall events in southeastern Brazil (Groisman et al., 2005; Marengo et al., 2009). A similar trend was reported by Shotyk et al. (2002) in a study of Holocene climate change, where elevated Ti concentrations indicated increased mineral input to the peatland. Importantly, the absence of correlation between Ti and Hg or Pb suggests that this Ti increase does not represent an additional atmospheric source of these contaminants but rather enhanced mineral particle transport driven by hydrological changes.

We propose that the increase in heavy precipitation events in recent decades has enhanced surface runoff from the slopes surrounding the INP peatland, transporting Ti-rich particulate matter into the site. This influx of mineral matter may also explain the decrease in bulk density observed in the INP profile. In contrast, the SONP peat profile did not exhibit a similar increase in Ti concentration, and our data indicate that Ti was among the main variables distinguishing the two areas (Figure 6). The influence of runoff events on peatland sediment input is strongly dependent on local topography and catchment area size (Price, 2011). Therefore, it is likely that the specific geomorphological and hydrological characteristics surrounding the SONP peatland rendered it less susceptible to the climate-driven changes observed at INP.

In contrast to the divergent behavior of Ti, our study revealed a significant increase in Hg concentrations within both INP and SONP peat profiles, particularly in the surface layers (Figures 4 and 5, Table 3). This similar increasing trend for Hg across both parks, despite their contrasting Ti dynamics, strongly suggests a regional-scale atmospheric source for Hg, rather than local runoff or geomorphological controls. These findings are consistent with documented increases in anthropogenic Hg emissions from industrial and urban centers in southeastern Brazil over recent decades, as well as long-range atmospheric transport of Hg from global sources.

Table 3. Comparison of mercury (Hg) and lead (Pb) concentrations and accumulation rates (AR) in peatlands from different regions of the world, including values from the present study (INP and SONP, southeastern Brazil).

REGION / PEATLAND	Hg (ng g^{-1})	Hg AR (µg m^{-2} yr^{-1})	Pb (µg g^{-1})	Pb AR (mg m^{-2} yr^{-1})	REFERENCE
Ontario, Canada	189	–	90	–	Givelet et al., 2003
Manitoba, Canada	120–187	405–832	–	–	Outridge et al., 2011
Xiaoxing'an, China	126–275	–	–	–	Liu et al., 2003
Switzerland	–	–	0.8–89.7*	–	Zaccone et al., 2009
Scotland	100–450	–	30–400	–	Yang et al., 2001
Guanabara Bay, Brazil	100–322	–	–	1–18	Covelli et al., 2012
–	38–177*	6–13	26–59	0.98	Coggins et al., 2006
Sweden	10–115	3.9	–	–	Osterwalder et al., 2017
Poland	–	–	91–190	–	Fiałkiewicz-Kozieł et al., 2011
INP (Brazil) – Lacerda & Ribeiro (2004)	20–420	36–120	40–70	8–40*	Lacerda & Ribeiro, 2004
INP (Brazil) – This study	**111–219***	**133–311***	**7–16***	**9.4–21***	**This study**
SONP (Brazil) – This study	**103–203***	**104–251***	**5–13***	**8.0–14***	**This study**

Notes: AR = accumulation rate. Values marked with an asterisk (*) have been rounded to the nearest unit. Dashes (–) indicate that the parameter was not reported in the original study. Hg accumulation rates (AR) are presented in µg m^{-2} yr^{-1} to ensure consistency with the majority of published studies; original values from references were converted where necessary. See original references for complete methodological details.

Overall, the Hg concentrations and accumulation rates measured in INP and SONP fall within the range of values reported for other ombrotrophic peatlands worldwide (Table 3). However, the Hg AR values in the present study (133–311 µg m^{-2} yr^{-1} at INP) are among the highest recorded, particularly when compared to European and North American sites. Conversely, Pb concentrations (5–16 µg g^{-1}) are relatively low, reflecting the absence of major local industrial sources within these protected Conservation Units.

These findings align with a well-documented global trend of rising Hg accumulation in peatlands since the early 20th century (Roos-Barraclough et al., 2002; Küttner et al., 2014; Grimaldi et al., 2008), which is widely attributed to the intensification of anthropogenic activities, including industrial emissions, fossil fuel combustion, and agricultural practices. Furthermore, sediment cores from Guanabara Bay (Silva et al., 2002), located in close proximity to our study sites, have revealed similar increasing

trends in Hg accumulation, suggesting a potential influence of human activities from the Rio de Janeiro metropolitan region.

While humification processes in peatlands are known to be influenced by atmospheric Hg deposition (Biester et al., 2003; Franzen et al., 2004; Perez-Rodríguez et al., 2015), our findings suggest that this factor may not be the primary driver of Hg accumulation in tropical peatlands. Notably, the Hg concentrations we observed in surface layers (140–200 ng g^{-1}) are comparable to those reported in temperate peatlands (Givelet et al., 2003; Outridge et al., 2011; Liu et al., 2003; Zaccone et al., 2009; Yang et al., 2001) (Table 3). This suggests that other factors, potentially related to regional Hg sources or biogeochemical processes, may play a more significant role in Hg accumulation within these tropical peatlands.

The observed increase in Hg AR within the INP peat profile after the 1950s (Figure 4) is likely linked to the intensification of human activities, particularly the increased use of fossil fuels and the expansion of industrial activities (Gębka et al., 2016; Yang et al., 2017; EEA, 2018). The Second World War and subsequent post-war industrialization period contributed to elevated atmospheric Hg levels due to the widespread use of mercury in various applications, including explosives and industrial processes. Additionally, regional factors such as gold mining in Brazil, especially the use of mercury amalgamation, have significantly contributed to Hg emissions, particularly in the Amazon region (Lacerda & Marins, 1997). These factors, combined with global atmospheric circulation patterns, have likely resulted in increased Hg deposition in our study areas.

Our findings are further supported by research on Hg accumulation rates in Guanabara Bay sediments (Covelli et al., 2012), which documented a significant increase in Hg AR after the 1960s, reflecting intensifying human activities in the Rio de Janeiro metropolitan region. Lacerda et al. (2004) reported a similar trend in Hg AR for lake sediments within the INP region, with a maximum value observed in the 1960s. This concurrence strengthens the evidence for a historical increase in Hg deposition within the area.

The results obtained in this study support the hypothesis that the INP region has been significantly impacted by climate change, particularly since the 1950s (Groisman et al., 2005; Marengo et al., 2009). The observed changes in hydrological processes likely played a key role in altering trace element accumulation patterns within the INP peatland. In contrast, the SONP profile did not exhibit a similar response, suggesting that climatic variations in this region may exert a weaker influence on metal accumulation. Indeed, our

PCA results show that Hg AR, Pb AR, Hg EF, and Pb EF were important factors distinguishing the two study sites (Figure 6).

The percentage of lithogenic Hg in the INP and SONP peat profiles (averaging 0.5% and 1.0%, respectively) falls within the lower range of values reported by Guedron et al. (2006) for French Guiana oxisols (10–25%). Although our lithogenic Hg percentages are lower than those reported for tropical oxisols, this difference is expected given that peatlands are dominated by organic matter accumulation rather than mineral weathering products. Lithogenic metals originate from the weathering of bedrock minerals, and their concentration is typically higher near the surface due to enhanced weathering processes (Grimaldi et al., 2008). This explains the observed decrease in the lithogenic fraction with depth in both peat profiles.

The Pb concentrations measured in this study (6.6–15.6 μg g^{-1}) are comparable to those reported for peatlands in temperate and boreal regions (1–10 μg g^{-1}) (Coggins et al., 2006; Givelet et al., 2003; Jackson et al., 2004; Pratte et al., 2013; Ukonmaanaho et al., 2004; Weiss et al., 2002; Zaccone et al., 2007). The increase in Pb concentrations observed in the SONP profile is likely linked to the historical use of leaded gasoline. Zhan et al. (2020) reported that anthropogenic Pb emissions from fossil fuel combustion contributed up to 75% of global atmospheric Pb contamination during the latter half of the 20th century. This timeframe coincides with the increased Pb levels observed in SONP, suggesting a potential influence of past gasoline usage on Pb accumulation in this peatland. Consistent with this interpretation, SONP samples were mostly located in the negative portion of PC2, a region strongly influenced by Pb (Figure 6). The phase-out of leaded gasoline in Brazil between 1989 and 1992 likely contributed to the subsequent decline in Pb emissions observed globally since the early 2000s (WHO, 2002; Li et al., 2012).

Our findings are consistent with Pb accumulation rates reported for peatlands in other regions (Coggins et al., 2006). Additionally, the presence of Pb enrichments in nearby surface sediments of the Guarapina Lagoon (Patchineelam et al., 1988) suggests a potential link between atmospheric Pb deposition and Pb accumulation in these tropical peatlands. Monteiro et al. (2012) reported an increase in Pb AR within Guanabara Bay sediments over the past century, further supporting the historical trend of rising Pb emissions.

The EF values for Pb in this study were considerably higher than those reported by Baptista Neto et al. (2000) for Guanabara Bay surface sediments. Based on the

classification system proposed by Yongming et al. (2006), our findings suggest "very severe enrichment" of Pb in the studied peatlands, particularly within the INP profile where EF values increased from the 1950s onwards (Figures 4 and 5). This contrasts with the SONP profile, where Pb EF remained relatively constant.

It is important to acknowledge limitations associated with EF calculations. The use of continental crustal averages in the absence of local background values can potentially lead to overestimations or underestimations of enrichment (Moura et al., 2019; De Vleeschouwer et al., 2007). Ideally, regional background values specific to the study area would provide a more accurate assessment of anthropogenic Pb influence. However, as highlighted by Arhin et al. (2017), rapid urbanization and industrialization processes make obtaining pristine background values increasingly difficult. Future research efforts should focus on establishing reliable regional background values for Pb in these tropical peatlands, which would allow for a more precise evaluation of anthropogenic Pb enrichment and its impact on the environment.

Despite these limitations, the consistent trends observed across multiple independent records (peatlands, lake sediments, and bay sediments) provide compelling evidence for increasing atmospheric deposition of Hg and Pb in southeastern Brazil over the past century, with important implications for the conservation of high-altitude peatlands in the Atlantic Forest biome.

CONCLUSION

This study analyzed geochemical records from two high-altitude ombrotrophic peatlands in southeastern Brazil—Itatiaia National Park (INP) and Serra dos Órgãos National Park (SONP) —to investigate the influence of anthropogenic activities and climate change on trace element accumulation (Hg, Pb, and Ti).

Both peatlands exhibited a significant increase in Hg concentrations and accumulation rates (AR) in surface layers, with INP showing some of the highest Hg AR values recorded globally (133–311 $\mu g\ m^{-2}\ yr^{-1}$). These increases coincide with the rise of industrial activity in Brazil from the 1950s onwards.

Low lithogenic contributions (Hg: 0.5–1.0%; Pb: 2.4–4.8%) and enrichment factors indicating "very severe enrichment" confirm that Hg and Pb are primarily of anthropogenic origin, linked to fossil fuel combustion, industrial emissions, and past use of leaded gasoline.

While INP showed increasing Pb concentrations, the SONP profile did not exhibit a similar increase after the phase-out of leaded gasoline in Brazil (1989–1992). This discrepancy may reflect regional variations in industrial development, local atmospheric circulation patterns, or site-specific geomorphological characteristics.

Ti concentrations increased in INP from the 1950s onwards, coinciding with intensified extreme rainfall events in southeastern Brazil. This suggests that climate-driven hydrological changes have enhanced mineral particle transport into the INP peatland, a trend not observed at SONP due to differences in topography and catchment area.

These findings are consistent with historical Hg and Pb emissions associated with post-World War II industrialization and demonstrate that even protected Conservation Units in Brazil are not immune to regional anthropogenic impacts. Future research should focus on: (i) establishing regional background values for trace elements to improve enrichment factor accuracy; (ii) investigating the potential ecological effects of metal deposition on local flora and fauna; and (iii) assessing the long-term impacts of climate change on peatland integrity and carbon storage in tropical high-altitude ecosystems.

ACKNOWLEDGEMENTS

We wish to thanks to the personnel of the “Parque Nacional de Itatiaia (PNI) e Parque Nacional da Serra dos Órgãos (PARNASO)” of the Instituto Chico Mendes de Conservação da Biodiversidade (ICMBio) for the support to develop these studies. E. Silva-Filho, would like to thank the Conselho Nacional de Desenvolvimento Científico e Tecnológico – CNPq (Research Productivity Fellowship, CNPq N º 06/2019) and FAPERJ research fellows: E. Silva-Filho (State Scientist Program – E-26/203.037/2007); A. Buch (Post-Doctoral Program Grade 10 – E-26/10204.459/2021)

Author contribution All authors (LFL, EDM, ACB, VTK, RADR, MCB and EVS-F) contributed to the study conception and design. The first draft of the manuscript was written by LFL and all authors commented on previous versions of the manuscript. All authors read and approved the final manuscript.

Funding This study was funded in part by the Coordenação de Aperfeiçoamento de Pessoal de Nível Superior – Brasil (CAPES) – Finance Code 001 and is an output of the INCT Continent-Ocean Materials Transfer (INCT-TMCOcean supported by Conselho Nacional de Desenvolvimento Científico e Tecnológico - CNPq Proc. No. 573.601/2008-2).

Data Availability The datasets generated during and/or analysed during the current study are available from the corresponding author on reasonable request.

Declarations

Competing Interests The authors declare that they have no known competing financial interests or personal relationships that could have appeared to influence the work reported in this paper. **Ethical approval** Not applicable.

Consent to participate Not Applicable.

Consent to publish This manuscript is for exclusive publication in Environmental Pollution.

REFERENCES

AMAP, UN Environment. Technical Background Report for the Global Mercury Assessment 2018; Arctic Monitoring and Assessment Programme: Oslo, Norway; UN Environment Programme, Chemicals and Health Branch: Geneva, Switzerland, 2019.

Anshari, G., Kershaw, A.P., Vvan der Kaars, S., 2001. A late pleistocene and Holocene pollen and charcoal record from peat swamp forest, Lake Sentarum Wildlife Reserve, West Kalimantan, Indonesia. Paleogeogr. Paleoclimatol. Paleoecol. 171, 213228. https://doi.org/10.1016/S0031-0182(01)00246-2

Appleby, P.G., Oldfield, F., 1983. The assessment of ^{210}Pb data from sites with varying sediment accumulation rates. Hydrobiologia 103, 29–35. https://doi.org/10.1007/BF00028424

Arhin, E., Mouri, H., Kazapoe, R., 2017. Inherent Errors in Using Continental Crustal Averages and Legislated Accepted Values in the Determination of Enrichment Factors (EFs): A Case Study in Northern Ghana in Developing Environmental Policies. J. Geogr. Nat. Disast. 7 (3), 204. https://doi.org/10.4172/2167-0587.1000204

Baptista Neto, J.A., Smith, B.J., McAllister, J.J., 2000. Heavy metal concentrations in surface sediments in a nearshore environment, Jurujuba Sound, Southeast Brazil. Environ. Pollut. 109, 1-9. https://doi.org/10.1016/S0269-7491(99)00233-X

Barel, J.M., Moulia V., Hamard, S., Sytiuk, A., Jassey, V.E.J., 2021. Come Rain, Come Shine: Peatland Carbon Dynamics Shift Under Extreme Precipitation. Front. Environ. Sci. 9, 659953 https://doi.org/10.3389/fenvs.2021.659953

Buch, A.C., Sisinno, C.L.S., Correia, M.E.F., Silva-Filho, E.V., 2018. Food preference and ecotoxicological tests with millipedes in litter contaminated with mercury. Sci. Total Environ. 633, 1173-1182. https://doi.org/10.1016/j.scitotenv.2018.03.280

Coggins, A.M., Jennings, S.G., Ebinghaus, R., 2006. Accumulation rates of the heavy metals lead, mercury and cadmium in ombrotrophic peatlands in the west of Ireland. Atmos. Environ. 40, 260-278. https://doi.org/10.1016/j.atmosenv.2005.09.049

Cooke, C.A., Curtis, J.H., Kenney, W.F., Drevnick, P., Sigel, P.E., 2021. Caribbean Lead and Mercury Pollution Archived in a Crater Lake. *Environ. Sci. Technol.* 6791. https://doi.org/10.1021/acs.est.1c06791.

Corella, J.P., Valero-Garcés, B.L., Wang, F., Martínez-Cortizas, A., Cuevas, C.A., Saiz-Lopez, A., 2017. 700 years reconstruction of mercury and lead atmospheric deposition in the Pyrenees (NE Spain). Atmos. Environ. 155, 97-107. https://doi.org/10.1016/j.atmosenv.2017.02.018

Covelli, S., Protopsalti, I., Acquavita, A., Sperle, M., Bonardi, M., Emili, A., 2012. Spatial

variation, speciation and sedimentary records of mercury in the Guanabara Bay (Rio de Janeiro, Brazil). *Cont. Shelf. Res*. 35, 29-42. https://doi.org/10.1016/j.csr.2011.12.003

Cutshall, N.H., Larsen, I.L., Olsen, C.R., 1983. Direct analysis of ^{210}Pb in sediment samples: self-absorption corrections. Nucl. Instrum. Methods Phys. Res. 20, 309-312. https://doi.org/10.1016/0167-5087(83)91273-5

De Jesus, L.D.F., Moreira, M.F.R.M., Azevedo, S.V., Borges, R.M., Gomes, R.A.A., Bergamini, F.P.B., Teixeira, L.R., 2018. Lead and mercury levels in an environmentally exposed population in the Central Brazil. Reports in Public Health. 34(2), 1-13. https://doi.org/10.1590/0102-311x00034417

De Vleeschouwer, F., Gérard, L., Goormaghtigh, C., Mattielli, N., Le Roux, G., Fagel, N., 2007. Atmospheric lead and heavy metal pollution records from a Belgian peat bog spanning the last two millenia: Human impact on a regional to global scale. Sci. Total Environ. 377, 282–295. https://doi.org/10.1016/j.scitotenv.2007.02.017

EEA – European Environmental Agency, 2018. Mercury in Europe's environment: A priority for European and global action. https://doi.org/10.2800/558803

EMBRAPA (Empresa Brasileira de Pesquisa Agropecuária), 2013. Sistema Brasileiro de Classificação de Solos. Centro Nacional de Pesquisa de Solo (Rio de Janeiro, RJ). Rio de Janeiro.

Fernandes, C.M, Mendes, J.C., Teixeira, P.A.D, Silva, L.F.R., 2022. Investigating assembly timing of Ediacaran Serra dos Órgãos batholith – Hints on prolonged magmatism at Ribeira belt, SE Brazil. J. S. AM. Earth Sci., 120, 104053. https://doi.org/10.1016/j.jsames.2022.104053

Fiałkiewicz-Kozieł, B., Smieja-Król, B., Palowski, B., 2011. Heavy metal accumulation 480 in two peat bogs from southern Poland. Studia Quaternaria, 28, 17-24.

Franzen, C., Kilian, R., Biester, H., 2004. Natural mercury enrichment in a minerogenic fend evaluation of sources and processes. J. Environ. Monit. 6, 466-472. https://doi.org/10.1039/B315767A

Gębka, K., Bełdowski, J., Bełdowska, M., 2016. The impact of military activities on the concentration of mercury in soils of military training grounds and marine sediments. Environ. Sci. Pollut. Res. Int. 23(22), 23103–23113. https://doi.org/10.1007/s11356-016-7436-0

Givelet, N., Roos-Barraclough, F., Shotyk, W., 2003. Predominant anthropogenic sources and rates of atmospheric mercury accumulation in southern Ontario recorded by peat cores from three bogs: comparison with natural "background" values (past 8000 years). J. Environ. Monit. 5, 935-949. https://doi.org/10.1039/B307140E

Grimaldi, C., Grimaldi, M., Guedron, S., 2008. Mercury distribution in tropical soil profiles related to origin of mercury and soil processes. Sci. Total Environ. 401, 121-129. https://doi.org/10.1016/j.scitotenv.2008.04.001

Groissman, P., Knight, R.W., Easterling, D.R., Karl, T.R., Hegerl, G.C., Razuvaev, V.N., 2005. Trends in intense precipitation in the climate record. J. Clim. 18, 1326-1350. https://doi.org/10.1175/JCLI3339.1

Guedron, S., Grimaldi, C., Chauvel, C., Spadini, L., Grimaldi, M., 2006. Weathering versus atmospheric contributions to mercury concentrations in French Guiana soils. Appl. Geochem. 21(11), 2010-2022. https://doi.org/10.1016/j.apgeochem.2006.08.011

Hausmann, B., Pelikan, C., Herbold, C.W., Köstlbacher, S., Albertsen, M., Eichorst, S.A., del Rio, T.G., Huemer, M., Nielsen, P.H., Rattei, T., Stingl, U., Tringe, S.G., Trojan, D., Wentrup, C., Woebken, D., Pester, M., Loy, A., 2018. Peatland *Acidobacteria* with a dissimilatory sulfur metabolism. *ISME J* 12, 1729- 1742. https://doi.org/10.1038/s41396-018-0077-1

ICMBio (Instituto Chico Mendes de Conservação da Biodiversidade), 2013a. Plano de manejo do Parque Nacional da Serra dos Órgãos - Rio de janeiro, Brazil.

ICMBio (Instituto Chico Mendes de Conservação da Biodiversidade), 2013b. Plano de manejo do Parque Nacional do Itatiaia - Rio de janeiro, Brazil.

Jackson, B.P., Winger, P.V., Lasier, P.J., 2004. Atmospheric lead deposition to Okefenokee Swamp, Georgia, USA. *Environ. Pollut*, 130, 445-451. https://doi.org/10.1016/j.envpol.2003.12.019

Küttner, A., Mighall, T., De Vleeschouwer, F., Mauquoy, D., Martínez Cortizas, A.M., Foster, I.D.L., Krupp, E., 2014. A 3300-year atmospheric metal contamination record from Raeburn Flow raised bog, south west Scotland. J. *Archaeol. Sci.* 44, 1-11. https://doi.org/10.1016/j.jas.2014.01.011

Lacerda, L.D. and Marins, R.V. (1997) Anthropogenic mercury emissions to the atmosphere in Brazil: The impact of gold mining. J. Geochem. Explor. 58, 223-229. https://doi.org/10.1016/S0375-6742(96)00068-4

Lacerda, L.D., 2003. Updating global Hg emissions from small-scale gold mining and assessing its environmental impacts. *Environ. Geol*. 43, 308-314. https://doi.org/10.1007/s00254-002-0627-7

Lacerda, L.D., Ribeiro, M.G., 2004. Changes in lead and mercury atmospheric deposition due to industrial emissions in southeastern Brazil. *J. Braz. Chem. Soc*. 15, 931-937. https://doi.org/10.1590/S0103-50532004000600022

Li, F., Ma, C., Zhang, P., 2020. Mercury Deposition, Climate Change and Anthropogenic Activities: A Review. *Frontiers in Earth Science*, 8, 316. https://doi.org/10.3389/feart.2020.00316

Li, Q., Cheng, H., Zhou, T., Lin, C., Guo, S., 2012. The estimated atmospheric lead Emissions in China, 1990-2009. *Atmos. Environ*. 60, 1-8. https://doi.org/10.1016/j.atmosenv.2012.06.025

Lindberg, S., Bullock, R., Ebinghaus, R., Engstrom, D., Feng, X.B., Fitzgerald, W., Pirrone, N., Prestbo, E., Seigneur, C., 2007. A synthesis of progress and uncertainties in attributing the sources of mercury in deposition. *Ambio.* 36(1), 19-32. https://doi.org/10.1579/0044-7447(2007)36[19:ASOPAU]2.0.CO;2

Liu, R., Wang, Q., Lu, X., Fang, F., Wang, Y., 2003. Distribution and speciation of mercury in the peat bog of Xiaoxing'an Mountain, northeastern China. *Environ. Pollut.* 124, 39-46. https://doi.org/10.1016/S0269-7491(02)00432-3

Lourençato, L.F., Caldeira, P.P., Bernardes, M.C., Buch, A.C., Teixeira, D.C., Silva-Filho, E.V., 2017. Carbon accumulation rates recorded in the last 150 years in tropical high mountain peatlands of the Atlantic Rainforest, SE-Brazil. Sci. Total Environ. 579, 439-446. https://doi.org/10.1016/j.scitotenv.2016.11.076

Lourençato, L.F., Bernardes, M.C., Buch, A.C., Silva-Filho, E.V., 2019. Lignin phenols in the paleoenvironmental reconstruction of high mountain peatlands from Atlantic Rainforest, SE-Brazil, *Catena*, 172, 509-515. https://doi.org/10.1016/j.catena.2018.09.013

Luby, S.P., Forsyth, J.E., Fatmi, Z., Rahman, M., Sultana, J., Plambeck, E.L., Miller, N.G., Bendavid, E., Winch, P.J., Hu, H., Lanphear, B., Landrigan, P.J. 2024. Removing lead from the global economy. *Lancet Planet Health.* 8, e966-e982. https://doi.org/10.1016/S2542-5196(24)00244-4

Malm, O., Pfeiffer, W.C., Souza, C.M.M., Reuter, R., 1990. Mercury pollution due to gold mining in the Madeira River Basin, Brazil. Ambios. 19, 11-15.

Marengo, J.A., Jones, R., Alves, L.M., Valverde, M.C., 2009. Future change of temperature and precipitation extremes in South America as derived from the PRECIS regional climate modeling system. *Int. J. Climatol*. 29, 2241-2255. https://doi.org/10.1002/joc.1863

Marins, R.V., Lacerda, L.D., Paraquetti, H.H.M., Paiva, E.C., Villas-Boas, R.C., 1998. Geochemistry of mercury in sediments of a sub-tropical coastal lagoon, Sepituba Bay,

743 southeastern Brazil. Bull. *Environ. Contam. Toxicol*. 61, 57-64.
744 https://doi.org/10.1007/s001289900729

745 Martinez-Cortizas, A., Garcia-Rodeja, E., Pontevedra Pombal, X., Novoa Munoz, J.C., Weiss,
746 D., Cheburkin, A., 2002. Atmospheric Pb deposition in Spain during the last 4600 years recorded
747 by two ombrotrophic peat bogs and implications for the use of peat as archive. Sci. Total Environ.
748 292, 33-44. https://doi.org/10.1016/S0048-9697(02)00031-1

749 Monteiro, F.F., Cordeiro, R.C., Santelli, R.E., Machado, W., Evangelista, H., Villar, L.S., Viana,
750 L.C.A., Bidone, E.D., 2012. Sedimentary geochemical record of historical anthropogenic
751 activities affecting Guanabara Bay (Brazil) environmental quality. *Environ Earth Sci*. 65, 1661-
752 1669. https://doi.org/10.1007/s12665-011-1143-4

753 Moteki, N., Adachi, K., Ohata, S., Yoshida, A., Harigaya, T., Koike, M., Kondo, Y.,
754 2017. Anthropogenic iron oxide aerosols enhance atmospheric heating. *Nat Commun* **8**, 15329
755 (2017). https://doi.org/10.1038/ncomms15329

756 Moura, I.F., Cesar, R.H.S., Barreto, A.A., Menezes, M.A.B.C., 2019. Evaluation of the factor of
757 enrichment of atmospheric particulate matter in the Campus of UFMG, Belo Horizonte. *Brazilian*
758 *Journal of Radiation Sciences*. 07-03A, 01-07. https://doi.org/10.15392/bjrs.v7i3A.894

759 Mróz, T., Lokas, E., Kocurek, J., Gasiorek, M., 2017. Atmospheric fallout radionuclides in
760 peatland from Southern Poland. J. Environ. Radioact. 175, 25-33.
761 https://doi.org/10.1016/j.jenvrad.2017.04.012

762 Nieboer, E., 1982. Lichens and mosses as monitors of industrial activity associated with uranium
763 mining in Northern Ontario, Canada-Part 3: accumulations of iron and titanium and their
764 mutual dependence. Environ. Pollut. B. 4, 181-192. https://doi.org/10.1016/0143-
765 148X(82)90051-9

766 Nimer, E., 1979. Climatologia do Brasil. Rio de Janeiro: IBGE, 422. (Recursos naturais e meio
767 ambiente). Osterwalder, S., Bishop, K., Alewell, C., Fritsche, J. Laudon, H., Åkerblom, S.,
768 Nilsson, M.B. (2017). Mercury evasion from a boreal peatland shortens the timeline for recovery
769 from legacy pollution. Sci Rep. 7, 16022. https://doi.org/10.1038/s41598- 17-16141-7

770 Osterwalder, S., Bishop, K., Alewell, C., Fritsche, J. Laudon, H., Åkerblom, S., Nilsson, M.B.,
771 2017. Mercury evasion from a boreal peatland shortens the timeline for recovery from legacy
772 pollution. Sci Rep., 7, 16022. https://doi.org/10.1038/s41598-017-16141-7

773 Outridge, P.M., Rausch, N., Percival, J.B., Shotyk, W., McNeely, R., 2011. Comparison of
774 mercury and zinc profiles in peat and lake sediment archives with historical changes in emissions
775 from the Flin Flon metal smelter, Manitoba, Canada. Sci.Total Environ., 409, 548-563.
776 https://doi.org/10.1016/j.scitotenv.2010.10.041

777 Pacyna, J.M., Pacyna, E.G., 2009. Changes of emissions and atmospheric deposition of mercury,
778 lead, and cadmium. Atmos. Environ. 43(1), 117-127.
779 https://doi.org/10.1016/j.atmosenv.2008.09.066

780 Page, S.E., Rieley, J.O., Shotyk, W., Weiss, D., 1999. Interdependence of peat and vegetation in
781 a tropical peat swamp forest. Phil. Trans. R. Soc. Lond. B. 354, 1885-1897.
782 https://doi.org/10.1098/rstb.1999.0529

783 Patchineelam, S.R., Leitao Filho, C.M., Kristotakis, K., Tobschall, H.J., 1988. Atmospheric Lead
784 Deposition into Guarapina Lagoon, Rio de Janeiro State, Brazil. In U. Seeliger, L.D. de Lacerda,
785 S.R. Patchineelam (Eds.) Metals in Coastal Environments of Latin America. Springer-Verlag,
786 Berlin. https://doi.org/10.1007/978-3-642-71483-2_8

787 Pérez-Rodríguez, M., Horák-Terra, I., Rodríguez-Lado, L., Aboal, J.R., Cortizas, A.M., 2015.
788 Long-Term (~57 ka) Controls on Mercury Accumulation in the Souther Hemisphere
789 Reconstructed Using a Peat Record from Pinheiro Mire (Minas Gerais, Brazil). Environ. Sci.
790 Technol. 49, 1356−1364. https://doi.org/10.1021/es504826d

Posit Team (2026). RStudio: Integrated Development Environment for R. Posit Software, PBC, Boston, MA. URL http://www.posit.co/.

Pratte, S., Mucci, A., Garneau, M., 2013. Historical records of atmospheric metal deposition along the St. Lawrence Valley (eastern Canada) based on peat bog cores. Atmos. Environ., 79, 831-840. https://doi.org/10.1016/j.atmosenv.2013.07.063

Price, k., 2011. Effects of watershed topography, soils, land use, and climate on baseflow hydrology in humid regions: A review. Progress in Physical Geography. 35(4) 465–492. https://doi.org/10.1177/0309133311402714

Roos-Barraclough, F., Givelet, N., Cheburkin, A.K., Shotyk, W., Norton, S.A., 2006. Use of Br and Se in peat to reconstruct the natural and anthropogenic fluxes of atmospheric Hg: a 10000-year record from Caribou Bog, Maine. Environ. Sci. Technol. 40, 188-194. https://doi.org/10.1021/es051945p

Roos-Barraclough, F., Martinez-Cortizas, A., García-Rodeja, E., Shotyk, W.A., 2002. A 14500 years record of the accumulation of atmospheric mercury in peat: volcanic signals, anthropogenic influences and a correlation to bromine accumulation. Earth Planet. Sci. Lett. 202, 435-451. https://doi.org/10.1016/S0012-821X(02)00805-1

Shotyk, W., Blaser, P., Gru¨nig, A., Cheburkin, A.K., 2000. A new approach for quantifying cumulative, anthropogenic, atmospheric lead deposition using peat cores from bogs: Pb in eight Swiss peat bog profiles. *Sci. Total Environ*. 249, 257-280. https://doi.org/10.1016/S0048-9697(99)00523-9

Shotyk, W., Rausch, N., Nieminen, T.M., Ukonmaanaho, L., Krachler, M., 2016. Isotopic composition of Pb in peat and porewaters from three contrasting ombrotrophic bogs in Finland: evidence of chemical diagenesis in response to acidification. *Environ. Sci. Technol*. 50, 9943-9951. https://doi.org/10.1021/acs.est.6b01076

Shotyk, W., Weiss, D., Heisterkamp, M., Cheburkin, A.K., Appleby, P.G., Adams, F.C., 2002. New peat bog record of atmospheric lead pollution in Switzerland: Pb concentrations, enrichment factors, isotopic composition, and organo lead species. *Environ. Sci. Technol*., 36, 3893-3900. https://doi.org/10.1021/es010196i

Shotyk, W., Weiss, D., Kramers, J.D., Martinez-Cortizas, A., Cheburkin, A.K., Emons, H., 2002. A peat bog record of natural, pre-anthropogenic enrichments of trace elements in atmospheric aerosols since 12 370 14C yr BP, and their variation with Holocene climate change. *Earth Planet. Sc. Lett.,* 199, 21-37. https://doi.org/10.1016/S0012-821X(02)00553-8

Sigel, A., Sigel, H., Sigel, R.K.O., 2017. Lead: Its Effects on Environment and Health (Metal Ions in Life Sciences Book 17) 1st Edition, Berlin, Boston, De Gruyt-er; 596 p. https://doi.org/10.1515/9783110434330

R Core Team (2026). R: A Language and Environment for Statistical Computing_. R Foundation for Statistical Computing, Vienna, Austria. doi:10.32614/R.manuals <https://doi.org/10.32614/R.manuals>. <https://www.R-project.org/>.

Rosa, P.A.S and Ruberti, E., 2018. Nepheline syenites to syenites and granitic rocks of the Itatiaia Alkaline Massif, Southeastern Brazil: new geological insights into a migratory ring Complex. Braz. J. Geol., 48(2), 347-372. https://doi.org/10.1590/2317-4889201820170092

Taminskas, J., Linkeviciene, R., Simanauskiene, R., Jukna, L., Kibirstis, G., Tamkeviciute, M., 2018. Climate change and water table fluctuation: implications for raised bog surface variability. Geomorphology. 304, 40–49. https://doi.org/10.1016/j.geomorph.2017.12.026

Taylor, M.P., Isley, C.F., Glover, J., 2019. Prevalence of childhood lead poisoning and respiratory disease associated with lead smelter emissions. *Environ. Int.,* 127, 340-352. https://doi.org/10.1016/j.envint.2019.01.062

Ukonmaanaho, L., Nieminen, T.M., Rausch, N., Shotyk, W., 2004. Heavy metal and arsenic

profiles in ombrogenous peat cores from four differently loaded areas in Finland. *Water. Air. Soil Pollut*. 158, 277-294. https://doi.org/10.1023/B:WATE.0000044860.70055.32

UNEP, 2013. Global Mercury Assessment 2013: Sources, Emissions, Releases and Environmental Transport. UNEP Chemicals Branch, Geneva, Switzerland

Vu, V.Q., 2011. ggbiplot: A ggplot2 based biplot_. R package version 0.55, <https://github.com/vqv/ggbiplot>.

Watari, T., Nansai, K., Nakajima, K., 2021. Major metals demand, supply, and environmental impacts to 2100: A critical review. *Resour. Conserv. Recy.* 164, 105107. https://doi.org/10.1016/j.resconrec.2020.105107

Wedepohl, K.H., 1995. The composition of the continental crust. *Geochim. Cosmoschim. Acta*. 59, 1217-1232. https://doi.org/10.1016/0016-7037(95)00038-2

Weiss, D., Shotyk, W., Kempf, O. 1999. Archives of atmospheric lead pollution. *Naturwissenschaften* 86, 262-275. https://doi.org/10.1007/s001140050612

Weiss, D., Shotyk, W., Boyle, E.A., Kramers, J.D., Appleby, P.G., Cheburkin, A.K., 2002. Comparative study of the temporal evolution of atmospheric lead deposition in Scotland and eastern Canada using blanket peat bogs. *Sci. Total Environ*. 292, 7-18. https://doi.org/10.1016/S0048-9697(02)00025-6

WHO - World Health Organization, 2002. Bulletin of the World Health Organization. 80 (10). Access: https://www.who.int/bulletin/archives/80(10)768.pdf

Wüst, R.A.J., Bustin, R.M., 2004. Late Pleistocene and Holocene development of the interior peat-accumulating basin of tropical Tasek Bera, Peninsular Malaysia. *Paleogeogr. Paleoclimatol. Paleoecol*. 211, 241-270. https://doi.org/10.1016/j.palaeo.2004.05.009

Yang, G., Wang, M., Chen, H., Liu, L., Wu, N., Zhu, D., Tian, J., Peng, C., Zhu, Q., He, Y., 2017. Responses of CO2 emission and pore water DOC concentration to soil warming and water table drawdown in Zoige Peatlands. *Atmos. Environ.* 152, 323-329. https://doi.org/10.1016/j.atmosenv.2016.12.051

Yang, H., Rose, N.L., Boyle, J.F., Battarbee, R.W., 2001. Storage and distribution of trace metals and spheroidal carbonaceous particles (SCPs) from atmospheric deposition in the catchment peats of Lochnagar, Scotland. *Environ. Pollut*. 115, 231-238. https://doi.org/10.1016/S0269-7491(01)00107-5

Yongming, H., Peixuan, D., Junji, C., Posmentier, E.S., 2006. Multivariate analysis of heavy metal contamination in urban dusts of Xi'an, Cent, China. Sci. Total Environ. 355, 176-186. https://doi.org/10.1016/j.scitotenv.2005.02.026

Zaccone, C., Cocozza, C., Cheburkin, A.K., Shotyk, W., Miano, T.M., 2007. Highly organic soils as "witnesses" of anthropogenic Pb, Cu, Zn, and ^{137}Cs inputs during centuries. *Water. Air. Soil Pollut*. 186, 263-271. https://doi.org/10.1007/s11270-007-9482-1

Zaccone, C., Santoro, A., Cocozza, C., Terzano, R., Shotyk, W., Miano, T.M., 2009. Comparison of Hg concentrations in ombrotrophic peat and corresponding humic acids, and implications for the use of bogs as archives of atmospheric Hg deposition. *Geoderma.* 148, 399-404. https://doi.org/10.1016/j.geoderma.2008.11.017

Zhan, T., Zhou, X., Cheng, W., He, X., Tu, L., Liu, X., Ge, J., Xie, Y., Zhang, J., Ma, Y., Qiao, Y., 2020. Atmospheric mercury accumulation rate in northeastern China during the past 800 years as recorded by the sediments o Tianchi Crater Lake. *Environ. Sci. Pollut. Res. Int*. 27(1), 571-578. https://doi.org/10.1007/s11356-019-06927-9

Zhang, Y., Hou, D., O´Connor, D., Shen, Z., Shi, P., Ok, Y.S., Tsang, D.C.W., Wen, Y., Luo, N., 2019. Lead contamination in Chinese surface soils: Source identification, spatial-temporal distribution and associated health risks. Crit. Rev. *Env. Sci. Tec.* 49(15), 1386-1423. https://doi.org/10.1080/10643389.2019.1571354

887 Zhang, Y.X., Jaegle, L., Thompson, L., Streets, D.G., 2014. Six centuries of changing oceanic
888 mercury. Glob. Biogeochem. Cycles. 28, 1251–1261. https://doi.org/10.1002/2014GB004939
889
890